

# Biobased Core-Shell Polymers

Baker W Kuehl, Lauren Brianna Burton, Jefferson Roberts-Dobie, Michael  
Forrester, Eric W Cochran

E-mail:

## Abstract

Here we identify a biobased polymer that shows promise as a replacement for soft acrylics used as rubbers for toughening engineering thermoplastics. Using glycerol-based monomers, a virtually untapped resource in terms of commercial volume and overall cost, a series of core-shell polymers were synthesized via seeded semi-batch emulsion polymerization. While core-shell polymers have been extensively studied, the majority of these have been of petroleum origins. This study illustrates that solketal acrylate can be used as a bioderived rubber and improve the ductility and impact strength of brittle engineering thermoplastics like PLA. Furthermore, we present a complete study of these impact-modified PLA composites' mechanical performance and morphology. The significance of these core-shell polymers is they are bioderived and polymerized in water indicating an easily adaptable and scalable process with minimal VOCs.

## Introduction

Polymer colloids have increased in popularity since World War II as the desire for a natural rubber latex was sought out.<sup>1</sup> Natural rubber latexes consist of a dispersion of polyisoprene particles stabilized by surfactants. Originally, styrene-butadiene rubber (SBR) latexes were

the focus; however, emulsion polymerization was recognized for its versatility and has led to a growth in production of a wide range of polymers. Emulsion polymerization is a well-known method for creating high molecular weight polymers due to the elimination of mass and heat transfer allowing for applications suitable for various industries.<sup>2,3</sup> This process involves only monomer droplets dispersed in an aqueous phase, which can result in well-defined morphologies and particle size dispersities. Emulsion polymerization is commonly used to develop polymer latexes to produce films, paints, and coatings. Furthermore, this technique can synthesize highly tailored core-shell polymers (CSPs), which can be generated using seeded semi-batch free radical emulsion polymerizations or a reversible addition-fragmentation chain transfer (RAFT) based approach using highly-engineered surfactants.<sup>4-9</sup> During free radical emulsion polymerization, RAFT-based polymeric surfactants act as seed stages, allowing existing particles to swell with new monomers.<sup>10</sup> CSPs are used in niche applications requiring high-end performance, such as drug delivery, petroleum refining, hydrophobic coatings, and impact-modified plastics.

High-impact strength plastics typically comprise a brittle matrix with small dispersed rubber pockets, allowing for energy dissipation through heat. However, enthalpic interactions must be combated for rubber-modified polymer blends to prevent aggregation.<sup>11,12</sup> Brittle thermoplastic matrices, such as poly(lactide) PLA, have poor impact strength and elongation, dramatically hindering their use as single-use plastic. Impact modifiers, like core-shell polymers, are often blended to impart crack resistance and flexibility.<sup>13</sup> Crack resistance is improved via similar mechanisms to how high-impact strength polystyrene (HIPS) eliminates its brittleness.<sup>14</sup> Polybutadiene (PB), dispersed as small rubber pockets in polystyrene (PS), can undergo cavitation promoting shear yielding of the matrix leading to the dispersion of mechanical stresses across a larger volume of the matrix. CSPs contain a rubbery core with a thermoplastic shell that is either miscible or graftable to the plastic matrix.<sup>15</sup> The core provides the energy dissipation mechanisms similar to PB in HIPS. The shell phase interacts with the matrix by physical or chemical coupling to ensure proper rubber dispersion

in the polymer matrix. Commercially, core-shell polymers primarily have lightly crosslinked cores of poly(butadiene-stat-styrene) or poly(butyl acrylate). These two rubbers have a low Tg that can efficiently dissipate mechanical energy. The shell comprises poly(methyl methacrylate) (PMMA) as it is highly miscible with many plastic matrices utilized commercially. However, an issue with highly-toughened thermoplastic is compostability. All the commercially available CSPs are derived from petroleum.

Polymer companies have sought to reduce carbon emissions to create a more sustainable future, leading to the popularity of molecules such as fatty acids and cyclic alcohol-derived monomers, which can be modified with vinyl groups and polymerized further. Due to the hydrophobic nature of the monomers, miniemulsion polymerization is necessary to create the polymer latex requiring large amounts of mechanical energy to prevent complete coagulation.<sup>16-18</sup> Solketal acrylate is a rubbery monomer that has not been explored much yet. It is derived from glycerol, a byproduct of biodiesel production, and acetone through acid-catalyzed transesterification. Solketal can be cleaved under acidic conditions, forming glycerol units, ultimately causing polymer degradation.<sup>19-21</sup> In this study, solketal (meth)acrylate polymers were synthesized using emulsion polymerization to generate core-shell particles for drug delivery. However, solketal acrylate has not been used as a rubbery core for engineering thermoplastic toughening. The study promotes solketal acrylate as a potential poly(n-butyl acrylate) substitute. The researchers synthesized three-layer core-shell particles with a slightly crosslinked rubbery core, a rigid shell phase, and a functional shell. The primary focus was on preparing these acrylic CSPs using seeded semi-batch emulsion polymerization and evaluating the performance of these reactive core-shell modifiers in PLA.

# Experimental Methods

## Materials

Chemicals and their sources:- DL-1,2 Isopropylidenglycerol (solketal), methyl acrylate, butyl acrylate, allyl methacrylate, butanediol diacrylate, sodium dodecyl sulfate, potassium persulfate, sodium bicarbonate, Tergitol-15-S-40-70%, and the enzyme lipase acrylic resin Candida Antarctica lipase (Novozyme 435) were purchased from Sigma-Aldrich. - Rhodapex EST-30, Sipomer COPS-1, and Sipomer AES-100 were purchased from Alfa Chemistry. All chemicals were used as received.

## Enzymatic Transesterification of Solketal Acrylate

Enzymatic transesterification was carried out using Solketal pre-monomer with excess methyl acrylate, lipase enzyme, and molecular sieves at 40°C for 24 hours, following the process by Goyal et al.

## Emulsion Polymerization

### Seed Stage

A process called seeded semi-batch emulsion polymerization was used to create CSPs. The process involved mixing 350 parts per hundred monomer (phm), 2 phm of sodium dodecyl sulfate, and 0.65 phm of 5wt% sodium bicarbonate in a three-neck round bottom flask equipped with a condenser, a mechanical agitator, and a feed port. The aqueous layer was stirred for five minutes before adding 100 phm of butyl acrylate. The mixture was then vigorously stirred for 30 minutes while slightly purging with argon. When the reaction was emulsified, the temperature was raised to 80°C. At this temperature, 0.65 phm of 2wt% KPS was injected into the reaction. The reaction was left to continue for 2.5 hours before it was cooled. The 20wt% solids emulsion was then filtered through a 50-micron sieve and stored.

## **Core Growth Stage**

A pre-emulsion was created by combining an aqueous layer made from 2.4 parts per hundred of Rhodapex EST-30, 0.5 parts per hundred of Tergitol 15-S-40-70%, 30 parts per hundred of deionized water, 0.2 parts per hundred of KPS-2wt%, 0.5 parts per hundred of Sipomer COPS-1, and 0.5 parts per hundred of Sipomer AES-100 with an oil layer consisting of 49.4 phm of butyl acrylate, 49.4 phm of solketal acrylate, 0.8 phm of allyl methacrylate, and 0.4 phm of butanediol diacrylate. This was done by adding the oil layer dropwise to the aqueous layer under vigorous stirring in a beaker equipped with a stir bar. In a three-neck round bottom flask equipped with an agitator, a condenser, and a feed port, 39 parts per hundred (phm) of the previously prepared seed latex, 60 phm of deionized (DI) water, 0.1 phm of KPS 2 wt%, 0.25 phm of sodium bicarbonate 5 wt%, and 0.3 phm of Rhodapex EST-30 were combined. The mixture was continuously purged with slight argon gas and heated to 80°C. Then, the pre-emulsion was slowly added to the pre-made seed latex over 90 minutes. The mixture was further reacted for an additional 45 minutes after the feeding period to create a core growth layer.

## **Shell Growth Stage**

An emulsion was created by mixing an aqueous layer consisting of 2.7 phm of Rhodapex EST-30, 0.5 phm of Tergitol 15-S-40-70%, 0.5 phm of Sipomer COPS-1, 0.5 phm of Sipomer AES-100, 0.2 phm of KPS-2wt%, 30 phm of DI water, and 0.25 phm of sodium bicarbonate 5wt% with an oil layer made up of 98.8 phm of methyl methacrylate, 0.8 phm of allyl methacrylate, and 0.4 phm of butanediol diacrylate. The oil layer was slowly added to the aqueous layer to create the emulsion while stirring the mixture in a beaker with a stir bar. After the emulsion was formed, it was fed into the core stage for 60 minutes and allowed to react for 30 minutes after the shell stage feeding.

## **Functional Shell Growth Stage**

An emulsion was created by mixing an aqueous layer containing 2.7 phm of Rhodapex EST-30, 0.5 phm of Tergitol 15-S-40-70%, 0.5 phm of Sipomer COPS-1, 0.5 phm of Sipomer AES-100, 0.2 phm of KPS-2wt%, 30 phm of DI water, and 0.25 phm of sodium bicarbonate 5wt%. The oil layer containing 98 phm of methyl methacrylate and 2 phm of glycidyl methacrylate was mixed and added dropwise into the aqueous layer while vigorously stirring. Once the emulsion was mixed, it was fed into the shell stage for 60 minutes and allowed to react for an additional 60 minutes. The reaction was then cooled down and filtered through a 50-micron sieve before storage.

## **Preparation of Polymer Blends**

Depending on the composition, the A+B polymer blends were fabricated by dry mixing a calculated polymer modifier with various amounts of PLA in a small blender. The mixture was then dried at 60 °C for two before melt blending. The polymer was then melt blended using a Process 11 twin screw extruder. The extrudate was cooled and prepared for injection molding. The blends were synthesized at 220 °C with a 45-second residence time at 250 RPM.

## **Preparation of Mechanical Property Test Specimens**

The extrudate made ASTM D256 IZOD bars and ASTM D638 Type 5 dogbones. A Haake MiniJet injection molder was used with the barrel temperature set to 240 °C and a mold temperature of 40 °C. The Ram pressure was set to 700 bar. Notches were then created under the ASTM D256 Specifications.

## **Mechanical Property Tests**

Uniaxial tensile tests were performed with an Instron 3367 Tensile Tester using a cross-head moving rate of 5mm/min. Impact Tests were conducted using a Tinius Olsen 527. The value

reported was represented as an average of over five specimens.

## Analysis of Microstructure

Microstructure analysis was performed on a 200kV JEOL 2100 Scanning/Transmission Electron Microscope. Each TEM specimen was ultra-microtomed at -70 °C in the whitened gauge region of the tensile bar. SEM was performed on the IZOD fracture surfaces using a FEI Quanta 250 FE-SEM.

## Particle Size Analysis

Measurements were conducted at 25°C using a Malvern Instruments Zetasizer Nano series instrument. Polymer dispersions were diluted to 1wt%. Z-average particle sizes were calculated using the average of three measurements.

## Dynamic Scanning Calorimetry

Modulated DSC was performed using a Discover 2500. The samples were dried at 100°C prior to undergoing a 2°C/min ramp from -100°C to 150°C

## Results and Discussion

Table 1: Summary of the Thermomechanical Properties of the Core-Shell Polymer Blends. Numbers in the Sample Code dictate the percentage of biobased polymer polymerized into the core.

Sample Code	Blend Thermomechanical Properties					Molecular Characteristics				Extruder Conditions	
	$\sigma$ (MPa)	$E$ (GPa)	$\epsilon_b$ (%)	$U_T$ (MJ/m <sup>3</sup> )	$E_{Frac}$ (J/m)	% GMA	% Crosslinker in Core	$\bar{r}_{ize}$ (nm)	$\bar{D}$	T°C	RPM
PLA	67 ± 2	2.5 ± 0.1	3 ± 1	1 ± 1	76 ± 11	NA	NA	NA	NA	NA	NA
CSP-50	56 ± 2	2.2 ± 0.1	58 ± 5	18 ± 1	140 ± 2	2.5	5	193	0.042	210	300
CSP-100	49 ± 2	2.0 ± 0.1	72 ± 8	26 ± 1	130 ± 2	2.5	5	193	0.042	210	300
CSP-50	58 ± 2	2.2 ± 0.1	68 ± 6	25 ± 2	150 ± 2	2.5	2.5	185	0.025	210	300
CSP-100	48 ± 2	2.1 ± 0.1	119 ± 14	35 ± 3	175 ± 5	2.5	2.5	185	0.025	210	300

Results

	Size (d.nm):	% Intensity:	St Dev (d.n...
<b>Z-Average (d.nm):</b> 210.8	<b>Peak 1:</b> 223.9	100.0	56.97
<b>Pdl:</b> 0.042	<b>Peak 2:</b> 0.000	0.0	0.000
<b>Intercept:</b> 0.940	<b>Peak 3:</b> 0.000	0.0	0.000
<b>Result quality :</b> Good			

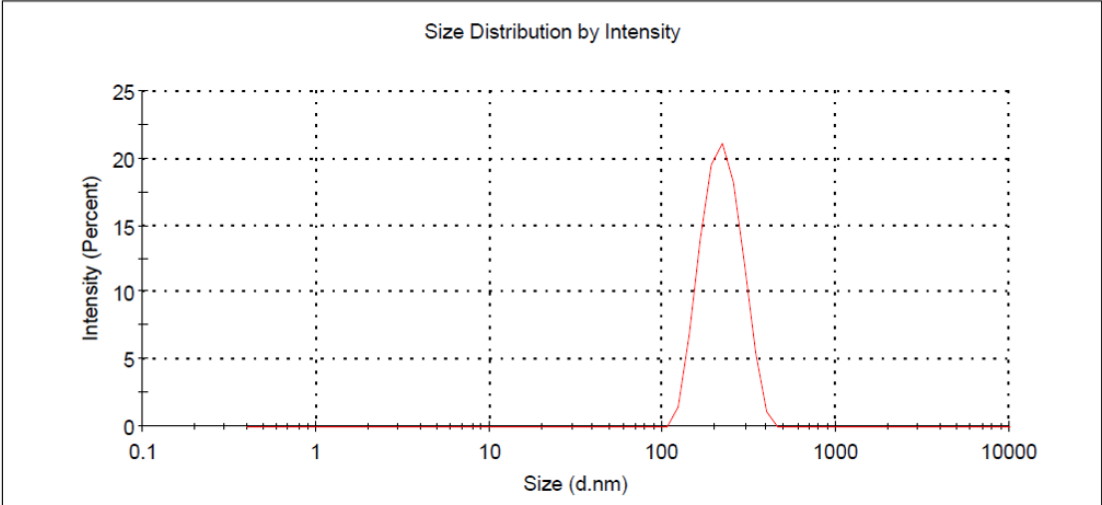


Figure 1: Representative DLS Particle Size Analysis of a Seeded Semi-Batch Emulsion Polymerized Core-Shell Polymer



All core-shell polymers were synthesized via seeded emulsion polymerization. Using a previously prepared seed latex avoided uncertainty in particle nucleation mechanisms and better batch-to-batch reproducibility. Polymerizations proceeded under monomer-starved conditions leading to a nearly instantaneous monomer conversion rate. A summary of CSPs can be viewed in Table 1. Molecular characteristics of the core-shell polymers can be viewed by showing particle size, dispersity, amount of crosslinker in the core, and percent glycidyl methacrylate copolymerized into the functional shell. Overall, particle sizes and dispersity did not vary much based on the loading of bioderived monomer indicating good incorporation into the soft core. DLS was used to obtain quantitative data about the particle sizes of the emulsions. DLS was used to ensure there was no secondary nucleation during the growth stages of the polymerization. According to figure 1, the emulsion polymerization proceeded without any secondary nucleation indicating an ideal environment for instantaneous polymerization.

After the formation of the CSP latex, a small sample was precipitated out of the latex and DSC was performed. Figure 4 presents the DSC thermograms for solketal acrylate cores produced by batch emulsion polymerization and semi-batch emulsion polymerization. The normalized heat flow, plotted against temperature, indicates significant differences in the thermal properties of the two samples. The Core Batch polymer shows a distinctly higher T<sub>g</sub> as compared to the semi-batch produced polymer. This difference in T<sub>g</sub> is influenced by the degradation of persulfate initiators, which generate local acid sites that can cleave solketal acrylate. In batch polymerization, the cleavage of the solketal ring results in the release of glycerol, a small molecule that disperses into the aqueous phase, minimizing its impact on the core T<sub>g</sub>. Conversely, in semi-batch polymerization, the glycerol remains confined within the rigid poly(methyl methacrylate) (PMMA) shell, inducing a self-plasticization effect that lowers the T<sub>g</sub>. This encapsulation increases the mobility of the polymer chains, thus modifying the thermal properties of the resulting polymer. Figure 3 illustrates the structural differences between polymer cores made from petroleum-based butyl acrylate and

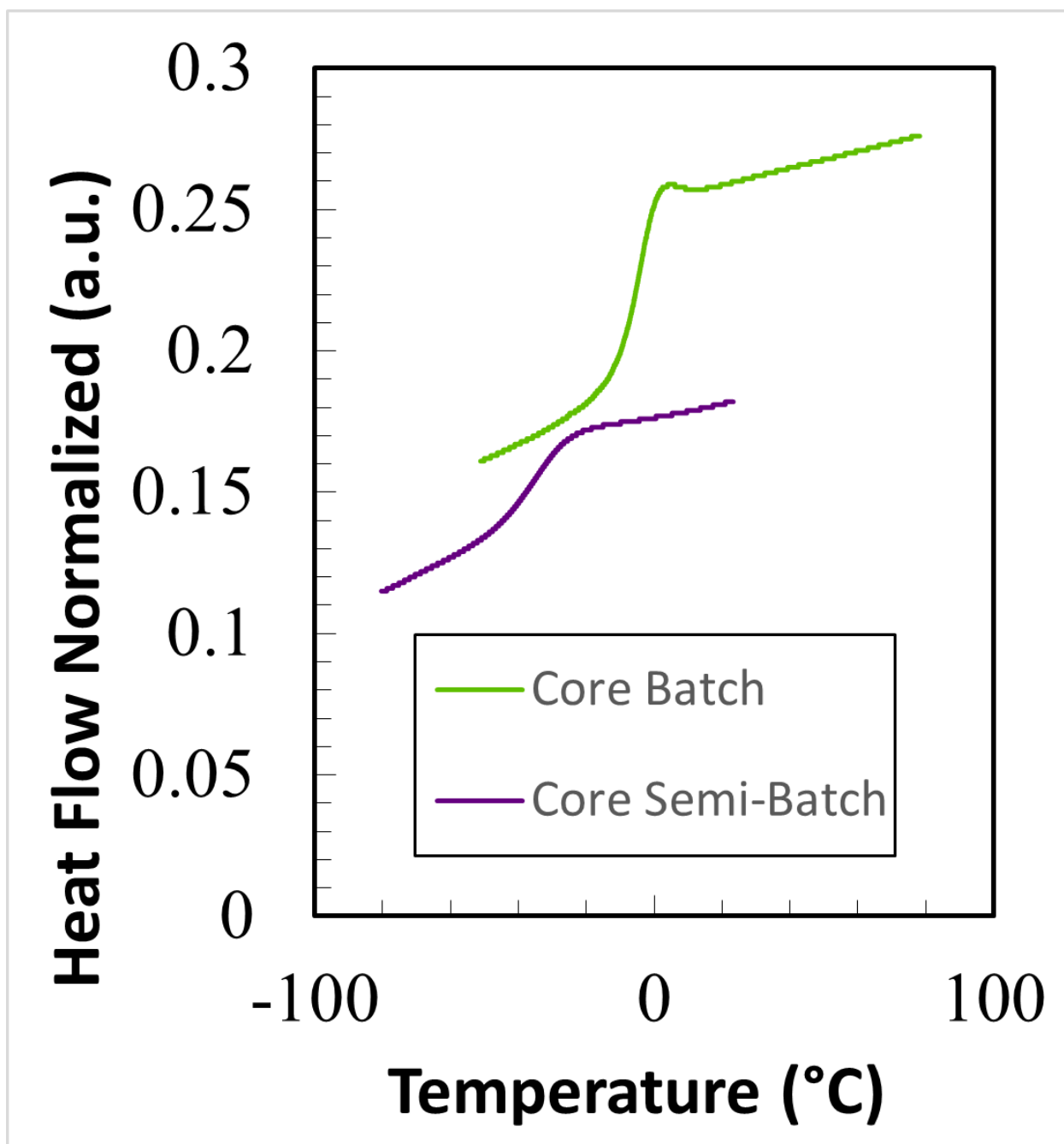


Figure 2: Representative DSC of the Varying Core-Shell Polymers at Different Loadings of Solketal Acrylate

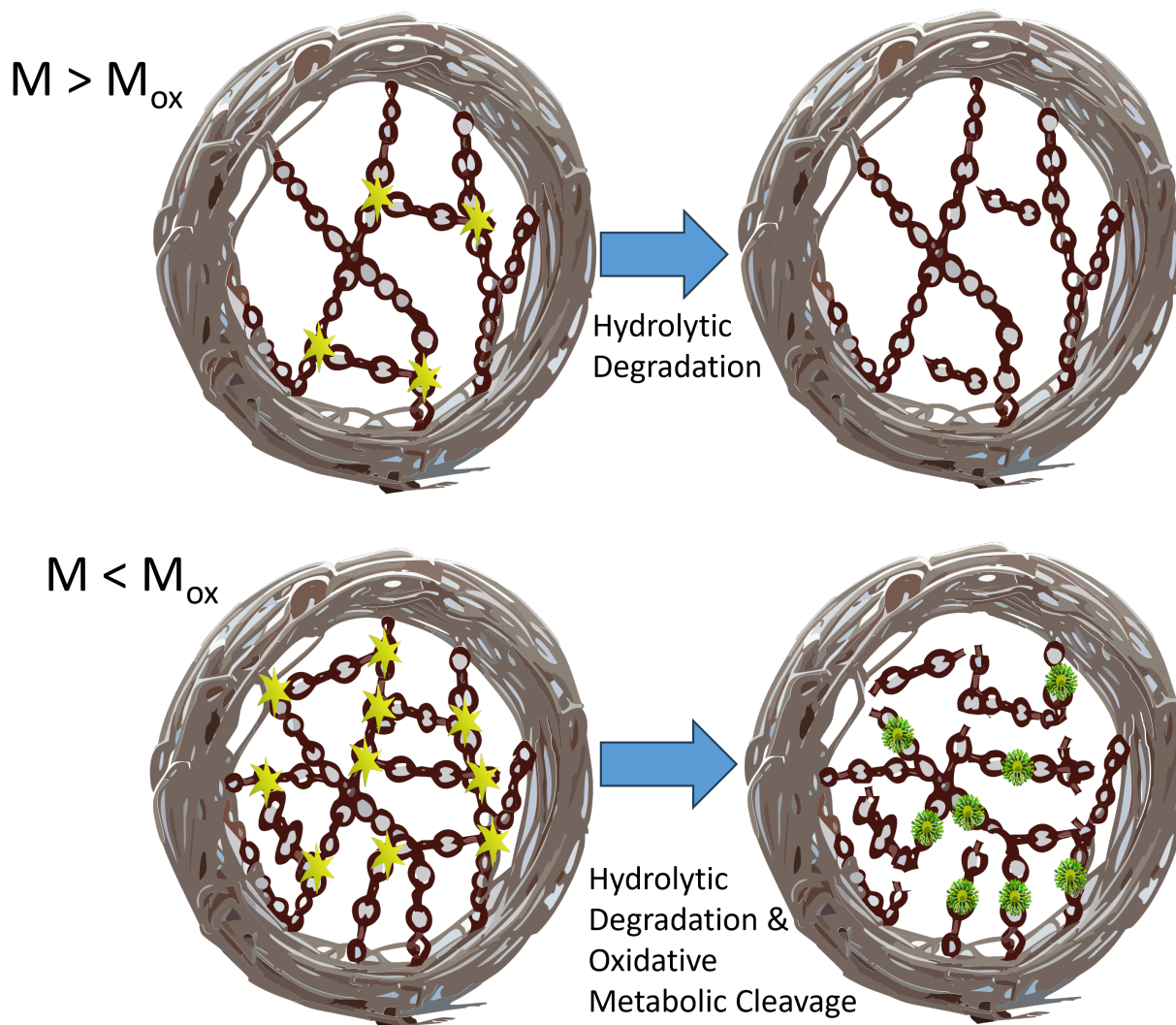


Figure 3: Schematic representation of polymer cores: (top) petroleum-based butyl acrylate core and (bottom) biobased solketal acrylate-derived core. The illustrations depict the initial polymerization stage (left) and the final core structure (right). Yellow stars indicate ester-based crosslinks, and green clusters indicate sites of oxidative metabolic cleavage.

biobased solketal acrylate. Polymers are challenging to degrade due to their high degree of polymerizations. Chain lengths larger than 1200 Da show a significant dropoff in the ability to undergo chain scission.<sup>22</sup> One of the challenges in designing a degradable CSP is to keep the molecular weight between crosslinks low enough to undergo metabolic cleavage while maintaining mechanical performance. The top panel represents the butyl acrylate core, showing the polymerization process transitioning from the initial to final stages. The yellow stars denote ester-based crosslinks, which are susceptible to hydrolytic cleavage. In contrast, the bottom panel shows the solketal acrylate-derived core undergoing a similar polymerization process. The ester-based crosslinks (yellow stars) also appear here, indicating sites vulnerable to hydrolytic cleavage. Additionally, green clusters in the final stage marks sites where biobased solketal acrylate can undergo oxidative metabolic cleavage, leading to significantly higher biodegradability. This structural distinction emphasizes the potential for biobased polymers to introduce unique properties and enhanced environmental benefits, attributed to the chemical nature of solketal acrylate and its interaction within the polymer system. Phase-separated polymers, like block copolymers, will show multiple glass transition temperatures for each polymeric phase. This is due to the energy penalty that must be paid for mixing polymers.<sup>23</sup> Core-shell polymers follow the same ideology in that a soft core and a rigid shell will display 2 distinct Tgs as each layer will not mix homogeneously together but are instead slightly grafted together to ensure microphase separation.<sup>24-26</sup> Figure 2 distinctly shows multiple glass transition temperatures corroborating the formation of core-shell polymers. CSP-50 and CSP-100 both show a rubbery low Tg corresponding to the core and a rigid high Tg corresponding to the shell. Rigid Tgs are fairly broad due to forming 2 polymer shells around the soft polymer core. Interestingly, CSP-0 shows 3 distinct Tgs indicating that the 1st and 2nd shells are completely immiscible with one another. This could be due to a difference in grafting efficiency of the 1st shell to the polymer core when solketal acrylate is present.<sup>27-30</sup> After the synthesis of the latex, the polymer was further spray dried which resulted in a small free-flowing powder shown in Figure S1. SEM micrograph of A)

showing spray-dried samples ensured the rubber particles could easily be dispersed into the extruder while B) shows a large agglomerate that likely will struggle to mix with the PLA matrix.

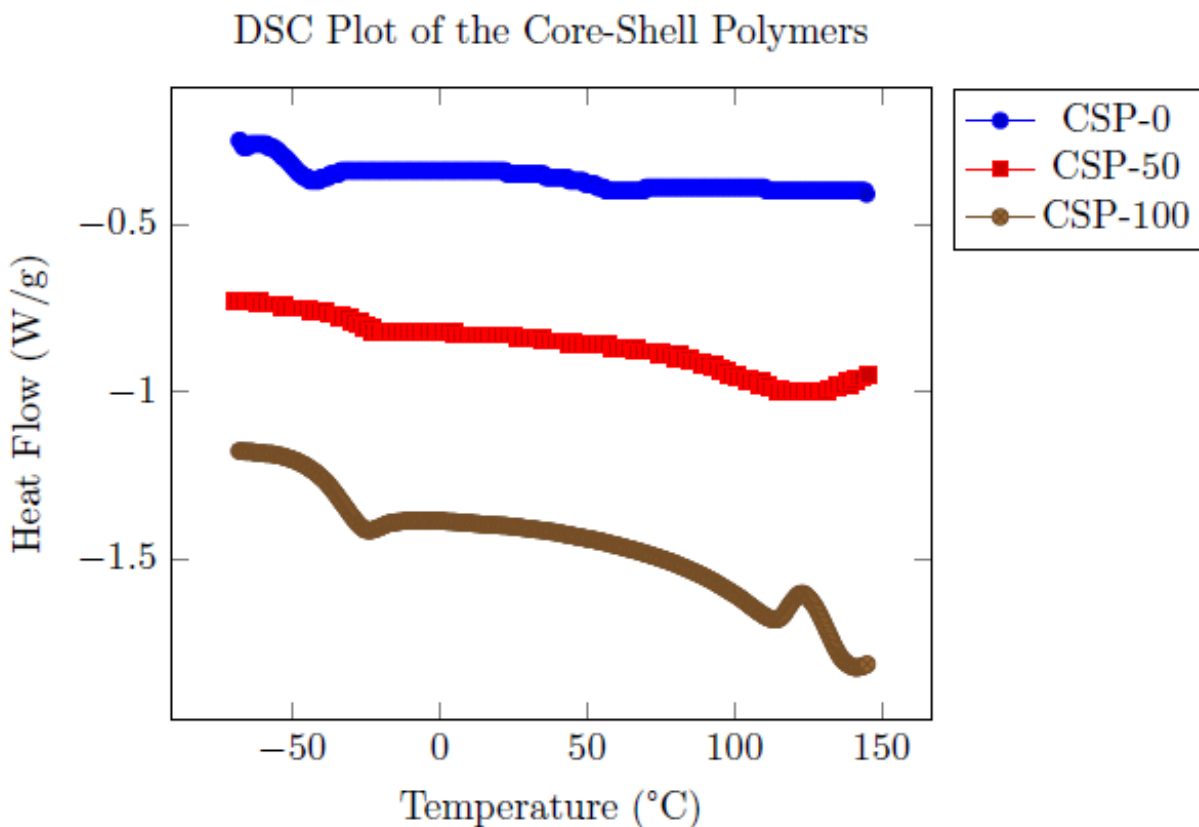


Figure 4: Differential Scanning Calorimetry (DSC) thermograms comparing the normalized heat flow of solketal acrylate synthesized via batch emulsion polymerization (Core Batch) and semi-batch emulsion polymerization (Core Semi-Batch). The thermograms demonstrate the two polymerization methods' distinct thermal behavior and glass transition temperatures (T<sub>g</sub>).

TEM and SEM were also performed on the core-shell polymer to confirm the core-shell structure shown in Figure 5. The TEM micrograph A) shows the obvious formation of the core-shell polymer structure. A dark core can be surrounded by a rough lighter stained shell with an average diameter that agrees closely with the DLS. SEM micrograph B) also shows the formation of spherical particles aggregated together with size corroborating with

the TEM and DLS. After confirmation of the formation of CSP, the particles were dispersed into PLA via a Process 11 twin-screw extruder. SEM and TEM figures of the PLA/CSP composites can be seen in figure6. It is generally believed the interfacial adhesion and dispersion of the rubber particles are extremely important in toughening thermoplastics. PMMA miscibility with PLA is generally believed to be miscible with PLA. Polyglycidyl methacrylate can also undergo a grafting mechanism forming ester bonds with the carboxylic chain ends of PLA further improving the interfacial adhesion and mechanical energy transfer between matrix and dispersed rubber. TEM micrographs indicate proper dispersion of the CSPs into the PLA matrix as evidenced by the evenly dispersed rubber pockets in the matrix. Stress concentration will be directly correlated to the dispersion of the rubber particles and SEM micrographs showing the IZOD impact surface can be used to correlate this effect. Figure 6A shows an extremely rough surface indicating high amounts of plastic deformation; however, the onset image in Figure 6A shows a pristine PLA surface indicating brittle failure. Further increasing the magnification shows CSP particles initiating shear bands in the PLA matrix resulting in fibrillation of the PLA matrix enhancing the toughness of the PLA. An increase in ductility of the PLA matrix results in a large increase in impact strength and stress whitening of the PLA matrix during mechanical deformation as seen in figure 7. Overall the formation of the CSP result in an order of magnitude increase in both the impact strength of PLA and the elongation.

## Conclusion

Our results show that biobased core-shell polymers can be synthesized via seeded emulsion polymerization and heavily modify a brittle PLA matrix. Tailoring the interfacial adhesion by altering the shell: core composition resulted in the formation of core-shell polymers. DLS, TEM, and SEM were used to corroborate the formation of core-shell particles and their dispersion in a PLA matrix that indicated ideal compatibility and adhesion between PLA



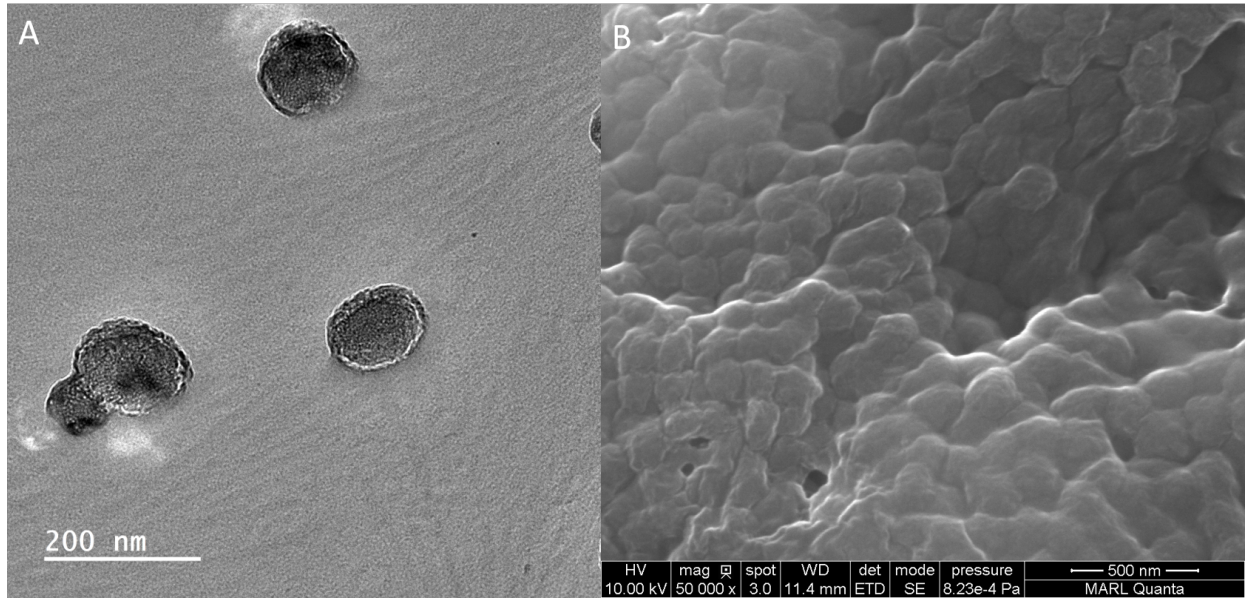


Figure 5: A) TEM micrograph of the Core-Shell Particles. B) SEM micrograph of the Core-Shell Particles.

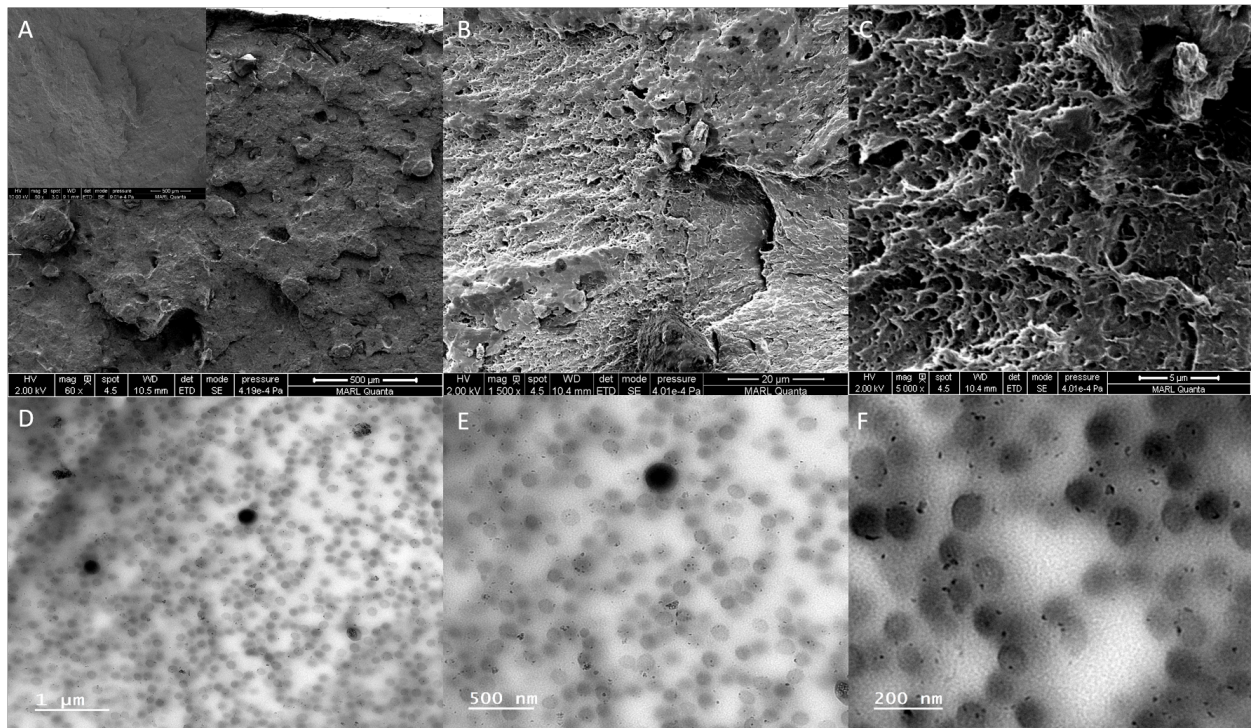


Figure 6: A), B), C) are all SEM micrographs at Low, Medium, and High MAGs respectively of CSP-modified PLA with an emphasis on the fracture surface of a Notched IZOD bar post-deformation. The onset in A is a micrograph of a Notched IZOD PLA surface. D), E), F) are all TEM images of the CSP dispersion in a PLA matrix

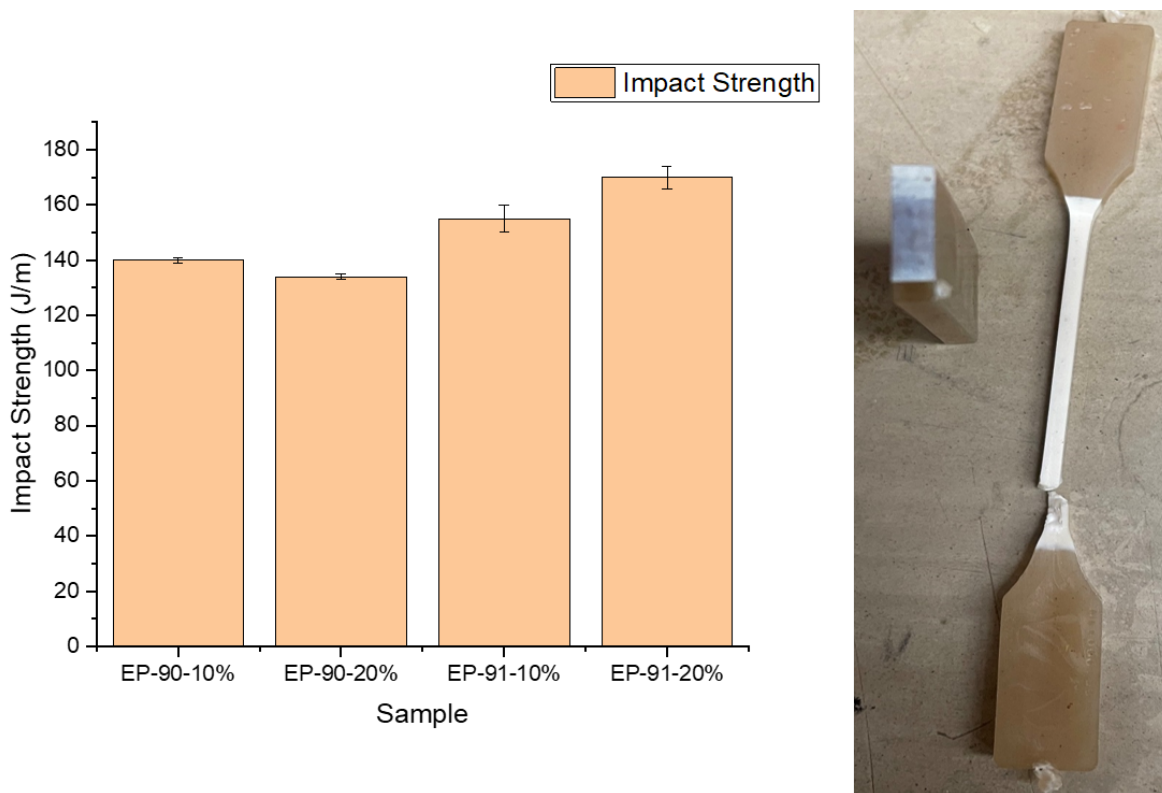


Figure 7: Impact Strength Data of the Polymer Blends

and the core-shell particles. SEM showed rough fracture surfaces indicating extreme plastic deformation, further identified as fibrillation of the PLA polymer chains. Employing these biobased core-shell polymers opens up avenues for toughened engineering thermoplastics that can retain their compostability.

## References

- (1) Badía, A.; Movellan, J.; Barandiaran, M. J.; Leiza, J. R. High Biobased Content Latexes for Development of Sustainable Pressure Sensitive Adhesives. *57*, 14509–14516.
- (2) Lovell, P. A.; Schork, F. J. Fundamentals of Emulsion Polymerization. *21*, 4396–4441.
- (3) Gao, W.; Li, C.; Li, J.; Zhang, Q.; Wang, N.; Abdel-Magid, B.; Qu, X. Effect of the Crosslinking Agent Content on the Emulsion Polymerization Process and Adhesive Properties of Poly(N-Butyl Acrylate-Co-Methacrylic Acid). *33*, 2031–2046.



- (4) Zhu, Y.; Gao, X.; Luo, Y. Core–Shell Particles of Poly(Methyl Methacrylate)-Block-Poly(*n*-Butyl Acrylate) Synthesized via Reversible Addition–Fragmentation Chain-Transfer Emulsion Polymerization and the Polymer’s Application in Toughening Polycarbonate. *133*.
- (5) Fu, N.; Li, G.; Zhang, Q.; Wang, N.; Qu, X. Preparation of a Functionalized Core–Shell Structured Polymer by Seeded Emulsion Polymerization and Investigation on Toughening Poly(Butylene Terephthalate). *4*, 1067–1073.
- (6) Chaduc, I.; Girod, M.; Antoine, R.; Charleux, B.; D’Agosto, F.; Lansalot, M. Batch Emulsion Polymerization Mediated by Poly(Methacrylic Acid) MacroRAFT Agents: One-Pot Synthesis of Self-Stabilized Particles. *45*, 5881–5893.
- (7) Zheng, Y.; Turner, W.; Zong, M.; Irvine, D. J.; Howdle, S. M.; Thurecht, K. J. Biodegradable Core Shell Materials via RAFT and ROP: Characterization and Comparison of Hyperbranched and Microgel Particles. *44*, 1347–1354.
- (8) Plessis, C.; Arzamendi, G.; Leiza, J. R.; Schoonbrood, H. A. S.; Charmot, D.; Asua, J. M. Seeded Semibatch Emulsion Polymerization of *N*-Butyl Acrylate. Kinetics and Structural Properties. *33*, 5041–5047.
- (9) Plessis, C.; Arzamendi, G.; Leiza, J. R.; Alberdi, J. M.; Schoonbrood, H. A. S.; Charmot, D.; Asua, J. M. Seeded Semibatch Emulsion Polymerization of Butyl Acrylate: Effect of the Chain-Transfer Agent on the Kinetics and Structural Properties. *39*, 1106–1119.
- (10) Zhu, Y.; Bi, S.; Gao, X.; Luo, Y. Comparison of RAFT Ab Initio Emulsion Polymerization of Methyl Methacrylate and Styrene Mediated by Oligo(Methacrylic Acid-*b*-Methyl Methacrylate) Trithiocarbonate Surfactant. *9*, 503–511.
- (11) Li, T.; Zhang, J.; Schneiderman, D. K.; Francis, L. F.; Bates, F. S. Toughening Glassy Poly(Lactide) with Block Copolymer Micelles. *5*, 359–364.

- (12) Zhao, H.; Liu, X.; Fu, N.; Zhang, Q.; Wang, N.; He, L.; Qu, X. Preparation of PBAS Core-Shell Structured Polymer by Seeded Emulsion Polymerization and Investigation in AS Resin Toughness. *125*, 3419–3428.
- (13) Sun, Y.; He, C. Biodegradable “Core-Shell” Rubber Nanoparticles and Their Toughening of Poly(Lactides). *46*, 9625–9633.
- (14) Zhang, S.; Zhu, S.; Feng, X.; Han, K.; Huan, Q.; Song, J.; Ma, Y.; Yu, M. Deformation and Toughening Mechanism for High Impact Polystyrene (HIPS) by Pressure-Induced-Flow Processing. *3*, 6879.
- (15) Aguiar, A.; González-Villegas, S.; Rabelero, M.; Mendizábal, E.; Puig, J. E.; Domínguez, J. M.; Katime, I. Core Shell Polymers with Improved Mechanical Properties Prepared by Microemulsion Polymerization. *32*, 6767–6771.
- (16) Demchuk, Z.; Mora, A.-S.; Choudhary, S.; Caillol, S.; Voronov, A. Biobased Latexes from Natural Oil Derivatives. *162*, 113237.
- (17) Bunker, S.; Staller, C.; Willenbacher, N.; Wool, R. Miniemulsion Polymerization of Acrylated Methyl Oleate for Pressure Sensitive Adhesives. *23*, 29–38.
- (18) Medeiros, A. M. M. S.; Machado, F.; Rubim, J. C.; McKenna, T. F. L. Bio-Based Copolymers Obtained through Miniemulsion Copolymerization of Methyl Esters of Acrylated Fatty Acids and Styrene. *55*, 1422–1432.
- (19) Mckenzie, A.; Hoskins, R.; Swift, T.; Grant, C.; Rimmer, S. Core (Polystyrene)–Shell [Poly(Glycerol Monomethacrylate)] Particles. *9*, 7577–7590.
- (20) Jesson, C. P.; Cunningham, V. J.; Smallridge, M. J.; Armes, S. P. Synthesis of High Molecular Weight Poly(Glycerol Monomethacrylate) via RAFT Emulsion Polymerization of Isopropylidenglycerol Methacrylate. *51*, 3221–3232.

- (21) Goyal, S.; Lin, F.-Y.; Forrester, M.; Henrichsen, W.; Murphy, G.; Shen, L.; Wang, T.-p.; Cochran, E. W. Glycerol Ketals as Building Blocks for a New Class of Biobased (Meth)Acrylate Polymers. *9*, 10620–10629.
- (22) Barbon, S. M.; Carter, M. C. D.; Yin, L.; Whaley, C. M.; Albright III, V. C.; Tecklenburg, R. E. Synthesis and Biodegradation Studies of Low-Dispersity Poly(Acrylic Acid). *Macromolecular Rapid Communications* **2022**, *43*, 2100773.
- (23) Zhang, X.; Sun, J.; Chen, Y.; Chen, Q.; Bai, L.; Gu, J.; Li, Z. Engineered Latex Particles Using Core–Shell Emulsion Polymerization: From a Strawberry-like Surface Pattern to a Shape-Memory Film.
- (24) Zhu, G.-Q.; Wang, F.-G.; Xu, K.-J.; Liu, Y.-Y. Emulsion Properties of Poly(n-Butyl Acrylate)/Poly(Methyl Methacrylate) Polymer with Core-Shell Structure. *25*, 3318–3320.
- (25) Li, Z.; Song, S.; Zhao, X.; Lv, X.; Sun, S. Grafting Modification of the Reactive Core-Shell Particles to Enhance the Toughening Ability of Polylactide. *10*, 957.
- (26) Plessis, C.; Arzamendi, G.; Leiza, J. R.; Schoonbrood, H. A. S.; Charmot, D.; Asua, J. M. Kinetics and Polymer Microstructure of the Seeded Semibatch Emulsion Copolymerization of N-Butyl Acrylate and Styrene. *34*, 5147–5157.
- (27) Guo, Y.; Sun, S.; Zhang, H. Modification of the Core–Shell Ratio to Prepare PB-g-(MMA-co-St-co-GMA) Particle-Toughened Poly(Butylene Terephthalate) and Polycarbonate Blends with Balanced Stiffness and Toughness. *4*, 58880–58887.
- (28) Li, P.; Zhu, J.; Sunintaboon, P.; Harris, F. W. New Route to Amphiphilic Core Shell Polymer Nanospheres: Graft Copolymerization of Methyl Methacrylate from Water-Soluble Polymer Chains Containing Amino Groups. *18*, 8641–8646.

- (29) Chen, P.; Cheng, Z.; Chu, F.; Xu, Y.; Wang, C. Fabrication of Polyacrylate Core–Shell Nanoparticles via Spray Drying Method. *18*, 124.
- (30) Gang, L.; Ting, W.; Maofang, H.; Tianming, G.; Xin, F. Effect of Ethyleneglycol Dimethacrylate Crosslinker on the Performance of Core-Double Shell Structure Poly(Vinyl Acetate-Butyl Acrylate) Emulsion. *132*.

## TOC Graphic

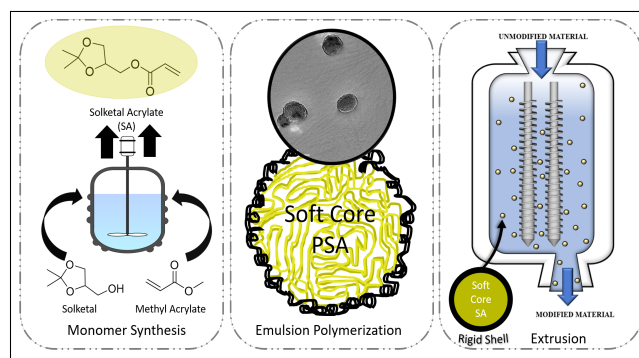


Illustration of the process to synthesize solketal acrylate monomer, followed by the synthesis of the core-shell polymer, and finally the incorporation of a biobased core-shell polymer into a PLA matrix.